

## MONITORING OF OIL PALM FIELDS USING UAV IMAGE USING GLCM METHOD

Deni Trianda Pitri<sup>1\*</sup>, Taufik<sup>2</sup>, Khairul Anwar<sup>3</sup>

Civil Engineering Study Program, Faculty of Engineering, Gunung Leuser Aceh University, Kutacane, Southeast Aceh

Email: [3denia@gmail.com](mailto:3denia@gmail.com), [taufiktanjung31@gmail.com](mailto:taufiktanjung31@gmail.com), [naufalkhairul80@gmail.com](mailto:naufalkhairul80@gmail.com).

### Abstract

Unmanned Aerial Vehicle (UAV) is a tool used to monitor oil palm land, from the beginning of the growth period so that it can be monitored which parts of the plantation land have fertile (growing perfectly), less fertile (growing but not perfect), or not growing at all. The orthophoto image produced by this UAV can be processed using Matlab, to distinguish fertile, less fertile and non-growing oil palm plants using the Gray Level Co-Occurrence Matrix (GLCM) method based on four parameters with gray degree directions of  $0^\circ$ ,  $45^\circ$ ,  $90^\circ$ , and  $135^\circ$  with 30 image samples. The four parameters are Contrast, Correlation, Energy or Entropy and Homogeneity. The results of image processing using the GLCM method are recalculated with statistics to map fertile, less fertile and non-growing areas. From the statistical results, the range value for the 00 contrast area is 7.7635, 450 contrast is 14.2758, 900 contrast is 8.2313, 1350 contrast is 12.5904. The 00 correlation range value is 0.1998, 450 correlation is 0.3625, 900 correlation is 0.1729 and 1350 correlation is 0.7310. The value range for 00 energy is 0.1137, 450 energy is 0.0965, 900 energy is 0.0988, 1350 energy is 0.4215. The value range for 00 homogeneity is 0.2964, 450 homogeneity is 0.2870, 900 homogeneity is 0.2553 and 1350 homogeneity is 0.2755

**Keywords:** UAV, Palm Oil, orthophotos, glcm

### INTRODUCTION

Image processing has a very wide spectrum of applications in various fields of life both in the fields of astronomy, biomedicine, biometrics, archaeology, archives and documents, industry and remote sensing using satellite image technology.

The use of satellite images has been widely carried out, especially to identify changes in the shape, area or condition of an area. This study utilizes satellite images using *Unmanned Aerial Vehicle* (UAV) to monitor oil palm plantations. The development of technology in the field of plantations is also increasing both in terms of planting, fertilizing, watering and harvesting produce. To get satisfactory yields, it is necessary to monitor the growth of oil palm plants from the beginning so that oil palm plants that are fertile, do not grow, or grow but are not healthy can be identified quickly and can be planted and fertilized again. For plantations with a small area, manual monitoring can be done. But it would be a problem if the area of

the crop was so large that it could not be monitored resulting in unsatisfactory yields.

To avoid these problems, monitoring technology is used. One of them is the *Unmanned Aerial Vehicle (UAV)*. UAV is a type of aircraft that is controlled by a remote control system device via radio waves. By using UAVs, data can be obtained at a relatively low cost, in a relatively fast time, and safely in various weather conditions. UAVs provide an efficient way to identify areas where seeds have not yet grown as expected in young oil palm plantations. It is also possible to achieve an initial estimate of the final result with constant monitoring. The use of UAVs has also been carried out for agriculture and regional vegetation, there is also to identify plants or tree characteristics. In this study, the focus will be on **Monitoring Oil Palm Fields Using Geospatial Orthophotos UAV Image Data Using the GLCM Method**. This research was conducted on community oil palm plantations in Salim Pipit Village, Babul Rahmah District, Southeast Aceh Regency.

The goal to be achieved in this study is to map geospatial image data from UAVs in terms of area area, plants that do not grow and plants that are less fertile so that they can be detected and then repaired quickly.

## **RESEARCH METHODOLOGY**

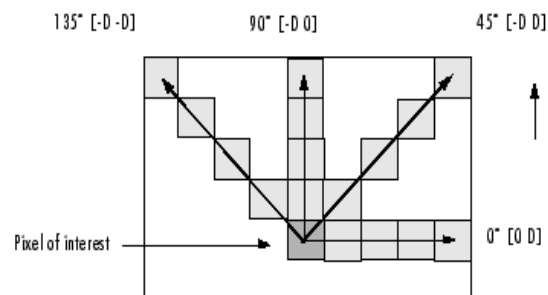
### **2.1 Common**

Monitoring of oil palm land in Indonesia is generally carried out manually. Manual methods can be done but are inefficient if the oil palm land is very large. In this study, oil palm land monitoring was carried out using UAVs. Where the use of this UAV aims to take palm oil orthophoto images. The resulting oil palm orthophoto image will be divided into three parts of the photo, namely a photo of a fertile, less fertile and non-growing oil palm. The oil palm land monitored is oil palm land owned by the community in Salim Pipit Village, Babul Rahmah District, Southeast Aceh Regency., using the dji 3 phantom type UAV. With the total area of the plantation is 4790 Ha. For data purposes, the area taken is 0.307 km<sup>2</sup> or about 30.7 Ha, with a flight altitude of 60 m, with a flight duration of 15 minutes. The camera used is a 3-axis gimbal with a camera resolution of 12 MP, the resulting photo format is Jpeg format. An orthophoto image of an oil palm plantation produced by a dji 3 panthom type camera is shown in Figure 2.1



Figure 3. 1 Palm orthophoto image

Existing palm orthophoto images will be processed to distinguish between fertile, underfertile and non-growing palm oil. To distinguish fertile, less fertile and non-growing oil palm, it is distinguished by four categories, namely contrast, correlation, energy or entropy and homogeneity. The four categories each have four directions of degrees, namely 0 degrees, 45 degrees, 90 degrees and 135 degrees. The four directions of degrees are illustrated in Figure 2.2.



The value of the co-occurrence matrix from each category will be reprocessed in order to obtain fertile, infertile and non-growing areas.

The software used in this thesis research is:

- a. Matlab 2015 software, is used to obtain parameter values from all four categories with the GLCM method to speed up the calculation process.
- b. SPSS software, is used to obtain the value of the range of fertile, less fertile and non-growing areas, so that the mapping of fertile, less fertile and non-growing areas is more accurate.

## 2.2 Image Segmentation

In image processing, sometimes we want to process only certain objects. Therefore, it is necessary to carry out an image segmentation process that aims to separate the object (*foreground*) from the *background*. In general, the output of the image segmentation result is in the form of a binary image where *the desired object (foreground)* is white (1), while *the background to be removed* is black (0). Similar to the process of improving image quality, the image segmentation process is also experimental, subjective, and depends on the goal to be achieved.

Image segmentation is an important stage in the process of pattern recognition. After the object is successfully segmented, then we can carry out the process of extracting image features. Characteristic extraction is a stage that aims to extract the characteristics of an object where the characteristics are used to distinguish between one object and another.

Feature extraction is the first step in classifying and interpreting images. This process is concerned with quantifying the characteristics of an image into a group of corresponding characteristic values. Feature extraction is divided into two parts, namely:

a. Extraction of first-order features

First-order feature extraction is a method of taking features based on the characteristics of the image histogram. The histogram shows the probability of the appearance of the grayness value of a pixel in an image. From the values on the resulting histogram, several first-order characteristic parameters can be calculated, including *mean*, *skewness*, *variance*, *curtosis*, and *entropy* [16].

1. Mean ( $\mu$ ) Indicates the measure of dispersion of an image

$$\mu = \sum_n f_n p(f_n) \dots\dots\dots (2.1)$$

where  $f_n$  is a grayish intensity value, while  $p(f_n)$  indicates the histogram value (the probability of the occurrence of the intensity in the image).

2. Variance ( $\sigma^2$ )

Shows the variation of elements on the histogram of an image

$$\sigma^2 = \sum_n (f_n - \mu)^2 p(f_n) \dots\dots\dots (2.2)$$

3. Skewness ( $\alpha_3$ )

Shows the relative degree of awkwardness of the histogram curve of an image.

$$\alpha_3 = \frac{1}{\sigma^3} \sum_n (f_n - \mu)^3 p(f_n) \dots\dots\dots (2.3)$$

4. Curtosis ( $\alpha_4$ )

Shows the relative degree of sharpness of the histogram curve of an image.

$$\alpha_4 = \frac{1}{\sigma^4} \sum_n (f_n - \mu)^4 p(f_n) - 3 \dots\dots\dots (2.4)$$

5. Entropy ( $H$ )

Indicates the size of the shape irregularity of an image.

$$H = - \sum_n p(f_n) \cdot 2_{\log p(f_n)} \dots\dots\dots (2.5)$$

b. Extraction of second-order features

In some cases, first-order features can no longer be used to recognize differences between images. In cases like this, we need to take second-order statistical features. One technique to obtain second-order statistical characteristics is to calculate the probability of a neighborly relationship between two pixels at a certain distance and angular orientation. This approach works by forming a

coordination matrix from the image data, followed by determining the characteristics as a function of the intermediate matrix.

Coocularity means co-occurrence, which is the number of events of one level of pixel value neighboring with one level of another pixel value within a certain distance ( $d$ ) and angular orientation ( $\theta$ ). Distance is expressed in pixels and orientation is expressed in degrees. The orientation is formed in four angular directions with angular intervals of  $45^\circ$ , namely  $0^\circ$ ,  $45^\circ$ ,  $90^\circ$ , and  $135^\circ$ . While the distance between pixels is usually set at 1 pixel.

A coocclusion matrix is a square matrix with the number of elements as many as the square of the number of pixel intensity levels in the image. Each dot ( $p,q$ ) on the coocracy-oriented matrix  $\theta$  contains the chance of a pixel event of value  $p$  neighboring pixels with value  $q$  at a distance  $d$  and the orientation  $\theta$  and  $(180-\theta)$ . After obtaining the coherence matrix, we can calculate the second-order statistical characteristics that represent the observed image. Haralick et al proposed different types of textural traits that can be extracted from cooccurrence matrices. In this module, the calculation of 6 second-order statistical characteristics is exemplified, namely *Angular Second Moment, Contrast, Correlation, Variance, Inverse Difference Moment, and Entropy*.

1. *Angular Second Moment (ASM)*

Indicates a measure of the homogeneity of the image.

$$ASM = \sum_i \sum_j \{p(i, j)\}^2 \dots\dots\dots (2.6)$$

where  $p(i,j)$  is the value in row  $i$  and column  $j$  in the cocurrency matrix.

2. *Kontrast (CON)*

Indicates the size of the spread (moment of inertia) of the elements of the image matrix. If it is located far from the main diagonal, the contrast value is large. Visually, the contrast value is a measure of the variation between the degrees of grayness of an image area.

$$CON = \sum_k k^2 [\sum_i \sum_j p(i, j)] \dots\dots\dots (2.7)$$

3. *Correlation (COR)*

Indicates the linear dependency measure of the grayish degree of the image so that it can provide clues to the presence of a linear structure in the image.

$$COR = \frac{\sum_i \sum_j (i, j) \cdot p(i, j) - \mu_x \mu_y}{\sigma_x \sigma_y} \dots\dots\dots (2.8)$$

Where:

$\mu_x$ : is the average value of the column element in the matrix  $p(i,j)$

$\mu_y$ : is the average value of the row element in the matrix  $p(i,j)$

$\sigma_x$ : is the standard deviation value of the element in the column  $p(i,j)$

$\sigma_y$ : is the standard deviation value of the element in the column  $p(i,j)$

4. *Variance (VAR)*

Showing variations in coexistence matrix elements. Images with a small grayish gradient will have a small variance as well.

$$VAR = \sum_i \sum_j (i - \mu_x)(j - \mu_y)p(i, j) \dots\dots\dots (2.9)$$

5. *Inverse Different Moment (IDM)*

Shows the homogeneity of the image with a degree of grayishness of the same kind. A homogeneous image will have a *large* IDM price.

$$IDM = \sum_i \sum_j \frac{1}{1+(i-j)^2} p(i, j) \dots\dots\dots (2.10)$$

6. *Entropy*

Indicates the size of the irregularity of the shape. The ENT price is large for images with even grayish gradients and is of little value if the image structure is irregular (varied).

$$ENT_2 = - \sum_i \sum_j p(i, j) \cdot 2_{\log p(i, j)} \dots\dots\dots (2.11)$$

**RESULTS AND DISCUSSION**

**3.1 Field Survey Results**

The field survey was carried out to collect satellite image data of oil palm in community plantations in Salim Pipit Village, Babul Rahmah District, Southeast Aceh Regency. This was done to take sample data of oil palm plantation areas that were fertile, less fertile and did not grow. The sample data taken is useful for further data processing. Sample data for fertile oil palm images were 10 pieces, less fertile areas were 10 pieces and no growing areas were also 10 samples. Sample data of oil palm images is shown in Table 3.1

The definition of fertile according to the large Indonesian dictionary is (1) can grow well (quickly grows), (2) good and healthy, (3) fat (contains a lot of substances that are good for plants). (4) live well (multiply, progress, grow and be strong). Defenini is infertile or infertile is (1) not growing well, (2) not developing well. While not growing is not living or dying.

**Table 3. 1 Sample Oil Palm Image Data**

Oil palm	Number of samples	Standard image	Image format
Sample 1	10	1	.jpg
Sample 2	10	1	.jpg
Sample 3	10	1	.jpg

while the image of the oil palm is shown in Figure 4.1



(c)

**Picture 3. 1 (a). Fertile Image Sample, (b). Less Fertile (c). Not Growing**

Figure 3.1 above is an image of an oil palm obtained from a DJI Phantom type drone. The image is the result of cropping from the original image, which will then be used as a sample for fertile, less fertile and non-growing areas, the image will be changed into a grayish image using the *Grey Level Coocurance Matrix (GLCM)* which informs the matrix value of the grayness image data and the value of the direction of the grayness degree of the image with 4 categories, namely contrast, correlation, energy and homogeneity. *Source code* The process of processing the original image into a grayish image using MATLAB.

**3.2 Results and Discussion of Image Processing**

The results of processing the original image to binary for the fertile, less fertile and non-growing regions are shown in Figure 4.2.



**Figure 3. 2 Oil Palm Grayish Image Results (a) fertile, (b) less fertile (c) not growing**

The grayish binary image above is an example of processing oil palm images from sample 1, picture 1, sample 2 picture 1 and sample 3 picture 1.

The results of the calculation of the grayish image matrix for sample 1, sample 2, and sample 3 can be seen in Appendix 1C. Testing for oil palm samples in fertile, less fertile and non-growing areas, with four categories, namely Contrast, Correlation, Energy, and Homogeneity, can be seen in Table 3.2.

**Table 3. 2 Grayness Degree GLCM Parameter Value with four Parameters**

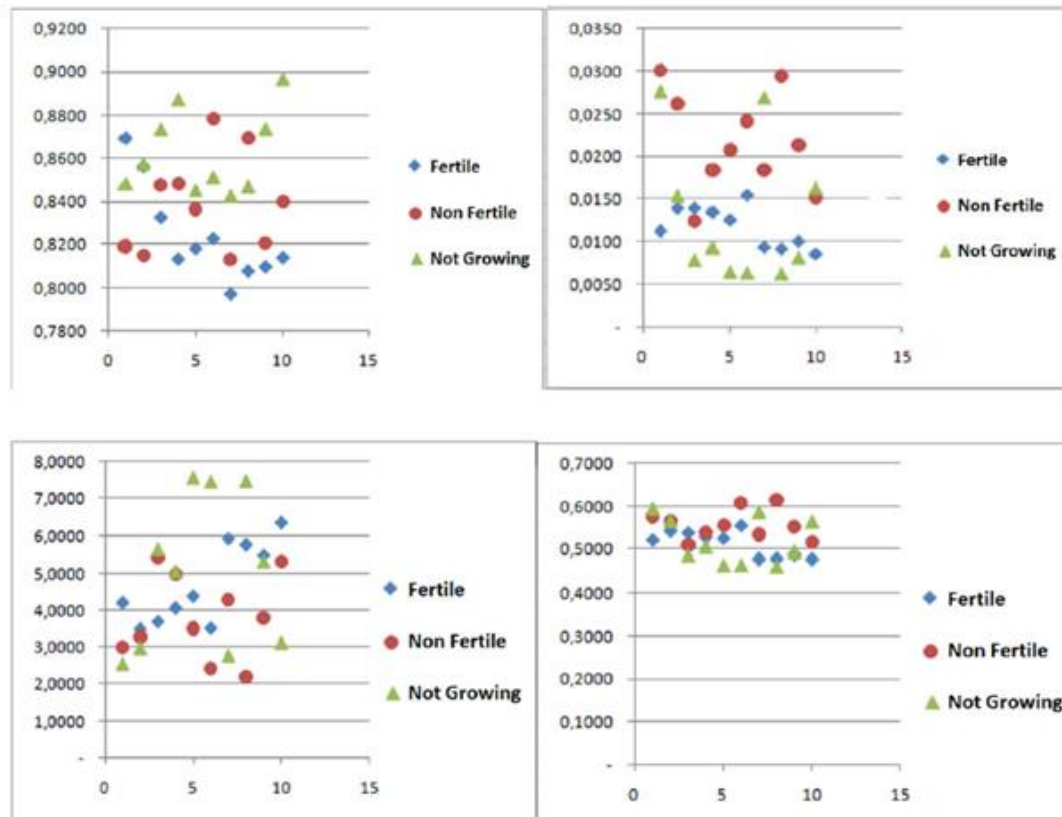
Sample 1												
Contrast				Correlation				Energy				Homogeneity
450	900	1350	00	450	900	1350	00	450	900	1350	00	450
10,0472	6,8559	9,9884	0,7130	0,5138	0,6684	0,5166	0,0120	0,0100	0,0120	0,0099	0,4739	0,4187
9,3698	5,9704	8,0541	0,7231	0,5767	0,7302	0,6358	0,0130	0,0112	0,0133	0,0115	0,4822	0,4437
10,1726	6,3753	8,0306	0,7116	0,5523	0,7196	0,6466	0,0135	0,0122	0,0144	0,0125	0,4807	0,4479
11,7994	7,8821	10,7783	0,7588	0,5539	0,7020	0,5920	0,0104	0,0085	0,0099	0,0083	0,4700	0,4200
7,9390	4,8454	5,9123	0,7985	0,5929	0,7513	0,6971	0,0142	0,0111	0,0134	0,0120	0,5204	0,4559
13,0478	8,7423	10,8496	0,7288	0,5055	0,6680	0,5891	0,0109	0,0088	0,0100	0,0090	0,4668	0,4067

12,3641	7,5605	9,4838	0,7685	0,5605	0,7312	0,6626	0,0111	0,0090	0,0114	0,0095	0,4720	0,4119
11,5312	8,2431	10,9348	0,7710	0,5676	0,6924	0,5903	0,0117	0,0093	0,0104	0,0091	0,4864	0,4230
9,6450	5,9453	8,2730	0,7458	0,5911	0,7477	0,6494	0,0130	0,0108	0,0129	0,0112	0,4897	0,4400
9,7920	6,2237	8,0863	0,7575	0,5668	0,7243	0,6424	0,0171	0,0141	0,0166	0,0147	0,5126	0,4630
<b>Sample 2</b>												
Contrast				Correlation								Homoc
450	900	1350	00	450	900	1350	00	450	900	1350	00	450
10,118	6,5785	10,4938	0,7305	0,5688	0,7178	0,5533	0,0141	0,0114	0,0134	0,0112	0,4922	0,4360
12,857	7,7991	10,9037	0,7353	0,5032	0,6944	0,5784	0,0128	0,0099	0,0118	0,0102	0,4828	0,4117
8,6627	4,9546	7,0484	0,8120	0,6641	0,8105	0,7266	0,0139	0,0112	0,0134	0,0123	0,4942	0,4340
13,5698	7,7146	11,2216	0,7802	0,6160	0,7802	0,6823	0,0087	0,0070	0,0092	0,0075	0,4646	0,3960
8,6970	5,1475	7,6481	0,7579	0,5427	0,7285	0,5987	0,0187	0,0149	0,0187	0,0156	0,5323	0,4690
15,4022	9,1384	13,9357	0,7365	0,5232	0,7134	0,5686	0,0124	0,0100	0,0128	0,0104	0,4675	0,4030
6,7094	3,8673	4,4486	0,7075	0,4668	0,6972	0,6464	0,0315	0,0254	0,0289	0,0272	0,5080	0,4840
9,0727	4,9308	6,3993	0,7930	0,5884	0,7821	0,7100	0,0221	0,0183	0,0213	0,0200	0,5217	0,4560
7,8728	4,2471	5,4531	0,7001	0,4544	0,7111	0,6222	0,0211	0,0170	0,0202	0,0183	0,5172	0,4420
8,3071	4,6664	6,2503	0,7883	0,6246	0,7951	0,7175	0,0154	0,0128	0,0155	0,0141	0,4968	0,4380
10,1268	5,9044	8,3803	0,7541	0,5552	0,7430	0,6404	0,0171	0,0138	0,0165	0,0147	0,4977	0,4370
10,5708	6,8644	9,0391	0,7477	0,5581	0,7135	0,6222	0,0127	0,0105	0,0124	0,0108	0,4855	0,4330
<b>Sample 3</b>												
Contrast				Correlation								Homoc
450	900	1350	00	450	900	1350	00	450	900	1350	00	450

3,0638	2,7582	3,5146	0,8180	0,6773	0,7197	0,6294	0,0355	0,0283	0,0301	0,0279	0,6224	0,5529
3,1047	2,5537	3,4791	0,8536	0,7316	0,7847	0,7028	0,0402	0,0325	0,0344	0,0312	0,6270	0,5569
1,1264	0,9071	1,3453	0,7454	0,6279	0,7099	0,5552	0,1224	0,1035	0,1080	0,1024	0,7512	0,6839
2,6383	2,4696	3,3684	0,8697	0,7328	0,7604	0,6577	0,0481	0,0350	0,0357	0,0335	0,6625	0,5662
2,7678	2,5827	3,4304	0,8564	0,7210	0,7507	0,6534	0,0484	0,0363	0,0367	0,0357	0,6511	0,5582
1,3464	1,1411	1,7921	0,8295	0,7589	0,8060	0,6821	0,0949	0,0831	0,0883	0,0800	0,7108	0,6548
2,0839	1,9429	2,7137	0,8999	0,8078	0,8307	0,7489	0,0590	0,0466	0,0464	0,4290	0,7001	0,6177
1,2330	1,0350	1,6173	0,8660	0,7932	0,8342	0,7305	0,1013	0,0865	0,0898	0,0824	0,7267	0,6699
2,3939	1,9580	2,8421	0,8793	0,8169	0,7268	0,0396	0,0396	0,0324	0,0340	0,0294	0,6477	0,5820
1,1644	0,9602	1,3671	0,8898	0,8013	0,8409	0,7706	0,1139	0,0895	0,0959	0,0894	0,7610	0,6689
2,0923	1,8309	2,5470	0,8508	0,7469	0,7764	0,6170	0,0703	0,0574	0,0599	0,0941	0,6861	0,6111

From the three samples tested, it can be seen that the contrast value for sample 1 is higher than the other two samples. This is because the color in sample 1 is brighter than the other samples. The correlation values of the three categories showed a linear dependency measure of the degree of grayness of the image for areas that did not grow larger than fertile and less fertile. For the value of entropy or energy the fertile area is small because it has an irregularity in the shape of the image, while for not growing and less fertile is large. Meanwhile, the homogeneity value for the fertile area is smaller than the other two areas. For more details, the difference can be seen in Graph 3.1, the direction of  $0^\circ$  for the four parameters, namely Contrast, correlation, energy or entropy and homogeneity.

**Graph 3.1 GLCM Paramator Values with Direction oO(a)Contras,(b)Corlation,(c)Energy,(d)Homogeneity**



### 3.2 Calculation of the area of oil palm

The standard palm oil image used in the image processing process is the original image taken from the DJI 3 Phantom type photo. The calculation of the area of oil palm is carried out using the threshold in the Matlab application. Below is the process of calculating the area of oil palm area.

```

clc;clear; close all;
image=imread('Fotosawit.jpg');
b=im2bw(image);
total=bwarea(b);
Subplot(1,2,1)
imshow(image);
title('RGB Mode Image');
Subplot(1,2,2)
imshow(b);
title('Binary Mode Image');
    
```

```
fprintf('\n Object Area Estimate is %0.4f\n',total);
```

The end of the calculation of the area of the oil palm image using the threshold is shown in figure 3.2.

The Estimated Area of the Object in binary count is 307101.6250. If converted into an area in  $\text{cm}^2$  and ha, the area is 66,020,415.49 $\text{cm}^2$ . It is assumed that the conversion of the value of 66.020.415.49  $\text{cm}^2$  to  $\text{km}^2$  is 0.307101625 $\text{km}^2$ , it is assumed that the conversion of the value of 0.307101625  $\text{km}^2$  in hectares of area area is about 30.7101625 ha. Therefore, the calculation of the area of the oil palm sample area calculated using matlab can be said to be the same as the calculation carried out manually.

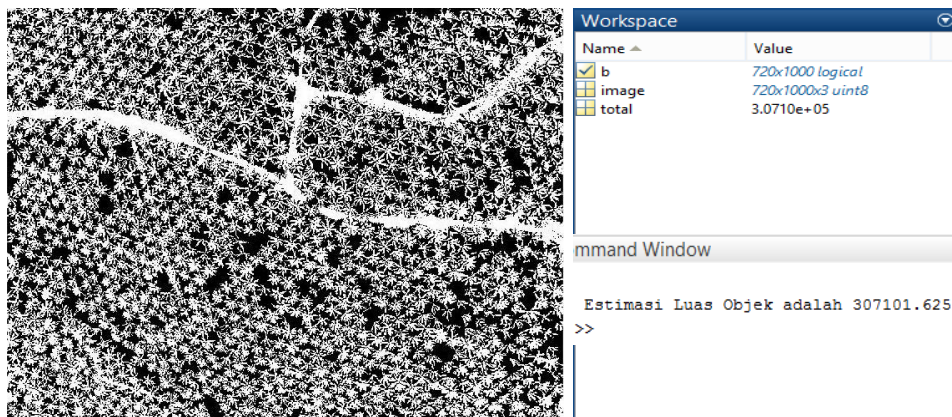


Figure 3.2 Binary image and area of oil palm image

## CONCLUSION

From the research that has been carried out, it can be concluded that:

Monitoring oil palm plantations using UAVs or drones can be done to map fertile, infertile and non-fast-growing areas and save operational costs and time.

The four parameters, namely contrast, correlation, energy and homogeneity, can map fertile, less fertile and non-growing regions, but the parameters that can identify fertile, less fertile and non-growing regions are contrast and correlation parameters. The area of the image sample area carried out using matlab with a threshold is 0.307  $\text{km}^2$

## REFERENCES

- R. Shofiyanti**, 2011. *Drone Technology for Mapping and Monitoring of Crops and Agricultural Land*, Inform. Pertan., vol. 20, no. 2, pp. 58–64.
- O. Guldogan, J. Rotola-pukkila, U. Balasundaram, T. Le, and K. Mannar**, 2016 *Automated Tree Detection and Density Calculation using Unmanned Aerial Vehicles*, Vcip2016, pp. 4–7.
- T. Moranduzzo and F. Melgani**, 2014. *Monitoring Structural Damages in Big Industrial Plants With Uav Images*, pp. 4950–4953,
- B. Emirul**, 2015 *Drone 1*. pp. 1–19,.
- J. J. Mitchell, N. F. Glenn, M. O. Anderson, R. C. Hruska, and A. H. Charlie**, 2012 *Unmanned Aerial Vehicle (UAV) Hyperspectral Remote Sensing for Dryland Vegetation Monitoring Hyperspectral Image and Signal Sensing*, 4th Work. Hyperspectral Image Signal Process., no. Ua V,.
- Valliappa Lakshmanan**, 2012 *Automating the Analysis of Spatial Grids A Practical Guide to Data Mining Geospatial Images for Human & Environ Mental Applications*, ISBN 978-94-007-4075-4 (eBook), published by Springer Dordrecht Heidelberg New York London,
- Olcay Guldogan, Jani Rotola-Pukkila, Uvaraj Balasundaram, Thanh-Hai Le, Kamal Mannar, Taufan Mega Chrisna, and Moncef Gabbouj**, 2016 *Automated Tree Detection and Density Calculation using Unmanned Aerial Vehicles*. 978-1-5090-5316-2/16/\$31.00 ©2016 IEEE, VCIP, Nov. 27 - 30, 2016, Chengdu, China
- Ni Made Rai Ratih C. Perbani, Deni Suwardhi**, 2014 *Development of Positioning and Navigation System Based on Unmanned Surface Vehicle (USV) System for Bathymetric Survey*, Itenas Journal of Engineering © LPPM Itenas | No.1 | Vol. XVIII ISSN: 1410-3125,
- Rochmad Muryamto, Waljiyanto, Untung Rahardjo, Gondang Riyadi, Ruli Andaru, Iqbal Taftazani, Wahyu Marta, and Annisa Farida**, 2016 *Creation of Maps and Geospatial Information System of Agricultural Land in Sentolo District, Kulonprogo Regency, Yogyakarta, Indonesian Journal of Community Engagement*, Vol. 01, No. 02, March.
- Agoes S. Soedomo and A. Indra Murti**, 2015 *BPN Single Map for Dizziness Quality of the Land Registration System (Problems, Opportunities and Alternative Solutions)*, Indonesian Journal of Geospatial Vol. 4, No.1.
- Jefferson R. Souza<sup>1</sup>, Caio C. T. Mendes, Vitor Guizilini, Kelen C. T. Vivaldini,**

**Adimara Colturato, Fabio Ramos and Denis F. Wolf, 2015**

*Automatic Detection of Ceratocystis Wilt in Eucalyptus Crops from Aerial Images* IEEE International Conference on Robotics and Automation (ICRA) Washington State Convention Center Seattle, Washington, May 26-30, 2015.

**Peggy A, Arie C,** *Next Generation Geospatial Information, from Digital Image Analysis to Spatio Temporal Databases, 2005*

**Hepi Handayani, Maria Regina Caeli,** *Study on the Calculation of the Number of Oil Palm Trees Using the Object-Based Classification Method* Publication at: <https://www.researchgate.net/publication/311770484>, October 2016.

**T. Acharya and A. K. Ray,** *Image Processing : Principles and Applications*, pp. 1–3, 2005.

**E. C. Processing et al.,** *Practicum ec4041 image processing and pattern recognition ec6041 image processing and advanced pattern recognition module 60 texture analysis*, pp. 1–13.

**S. Kusumadewi,** *Artificial Neural Networks using MATLAB & EXCEL LINK*, in *Intelligent Computing and Systems*, 2004th ed., vol. 1, GRAHA ILMU, 2004, p. 408.

**J. Kim, B. Kim, S. Savarese, and A. Arbor,** *Comparing Image Classification Methods : K-Nearest-Neighbor and Support-Vector-Machines* Pp. 133–138.

**P. Mohanaiah, P.sathyanarayana, L. Gurukumar,** 5, May 2013 *Image Texture Feature Extraction Using GLCM Approach, International Journal of Scientific and Research Publications*, Volume 3, Issue 1 ISSN 2250-3153

**Jonatan Sarwono,** 2009 *Statistics are an easy complete guide to learning Statistical Computing Using Spss*, Andi Yogya Karta, 2009.

**Hadi Kasumah (2017)** *Analysis of Bearing Capacity and Land Subsidence on Palm Foundations (Case Study: Construction of Shophouses on Jl Pelabuhan II, Sukabumi City)*

**Hardiyatmo, 2006.** *Foundation Techniques 1 & 2*. Third edition. Yogyakarta: Beta Offset

**Krisna Susanti zalukhu (2019)** *Analysis of the stability of soil retaining walls on the tarutung-sibolga section sta 23+250 –sta 23+270*

**K. Basah Suryolelono, 2002.** *Foundation Engineering Part II*. Yogyakarta: Gadjah Mada University.

**Muhammad Gupi, 2008.***Planning of the Kuantan River Cliff in Kuantan Singingi district uses a concrete pavement type.* Pekanbaru: Thesis of the Faculty of Engineering , Department of Civil Engineering, Islamic University of Riau.

**Government Regulation of the Republic of Indonesia Number 06/PRT/M/2015.**  
Article 3 paragraph 1 and In Article 6 paragraphs 1 to 3